SpaceOps-2025, ID # 174

Network and operational analysis of an optical ground station service for low Earth orbit and lunar communications

Marcus Birch[a]*, Hanna Sundberg[a], Marc Sans[a], Francis Bennet[b], Pritimoy Podder[a], Anton Bjöörn[a], Petrus Hyvönen[a]

[a] *Swedish Space Corporation, Torggatan 15, Lastkaj B, SE-106 91, Stockholm, Sweden*

[b] *Advanced Instrumentation Technology Centre, Research School of Astronomy and Astrophysics, Australian National University, Canberra, ACT 2611, Australia*

* Corresponding Author: marcus.birch@sscspace.com

Abstract

The Swedish Space Corporation (SSC) is developing a commercial optical ground segment service and is currently commissioning two optical ground stations (OGSs) in Australia and Chile. The development is carried out as a project within the European Space Agency ARTES programme. The SSC optical network will offer a high data rate direct-to-Earth service for low Earth orbit (LEO) satellites using free-space optical communications, pioneering one of the first commercial services of this kind. Unlike the deterministic approach of traditional radio satellite communication, this network will employ a flexible concept-of-operations to mitigate outages caused by cloud cover. In this paper, analysis provides estimations of data volume and latency for LEO downlinks, showing that a sparse network of two OGSs can provide over 200 GB/day with existing optical terminals. The results also present relative improvement, e.g. 40% greater data throughput, from forming a collaborative network with the Australian National University's (ANU) OGS in Canberra. Partnership with the ANU is being supported by the Australian Space Agency's Moon-to-Mars initiative, which is also supporting upgrades to ANU's OGS for high photon efficiency lunar links. Therefore, a preliminary analysis of a collaborative optical ground segment for lunar spacecraft is presented with estimations of expected uptime.

Keywords: Free-Space Optical Communication, Communications Architectures and Networks, Optical Ground Station, Atmosphere

1. Introduction

Free-space optical communication can provide secure and high data rate direct-to-Earth (DTE) links without spectrum licensing constraints, at the cost of atmospheric outages. Although building a diverse network of optical ground stations (OGSs) is a known solution to overcoming clouds, implementing this commercially has been prohibitively complex so far. The Swedish Space Corporation (SSC) is currently deploying a network of two OGSs to demonstrate the capability of this technology and offer one of the first commercial optical ground segment-as-a-service. SSC's Network of Optical stations for Data transport to Earth from Space (NODES) project, supported by the European Space Agency (ESA) and with funding support from Swedish National Space Agency (SNSA), has been ongoing since 2022 to develop this service. Operations will support direct-detection on-off keying links up to 10 Gbps, including both the Consultative Committee for Space Data Systems (CCSDS) Optical On-Off Keying (O3K) and Space Development Agency (SDA) Optical Communications Terminal standards [1, 2, 3]. The bi-static design in both stations incorporates an uplink beacon around 1590 nm for the CCSDS O3K standard, whereas a full-duplex beaconless capability is followed for the SDA (with interchangeable 1553 nm and 1536 nm transmit/receive wavelengths).

Capabilities of the two OGSs are being rolled out incrementally over 2025 and 2026, with this period serving as a demonstration phase for the service. OGS1, at the Western Australia Space Centre (WASC), was manufactured by Cailabs and is pictured in Figure 1 after installation. The baseline configuration of OGS1 supports CCSDS O3K and the station will be further upgraded to support SDA in 2026. The installation of the second station, OGS2, will begin in Q3 2025 in Santiago, Chile, which is being manufactured by Safran Data Systems. Both stations will be co-located with SSC sites from its global radio frequency ground station network and have been chosen for their high cloud-free availability, existing network connectivity, and on-site staff. Both OGSs are also automated turnkey systems designed for minimal operator involvement, and some of the first turnkey OGSs to be procured from this emerging market of commercial manufacturers.

Figure 1: SSC's OGS1, located at the Western Australia Space Centre near Dongara, Australia. Picture taken in February 2025.

SSC is collaborating with the Australian National University (ANU) and investigating the inclusion of their recently commissioned Quantum Optical Ground Station (QOGS) for a combined and improved service for specific missions. Unlike the SSC OGSs, QOGS functions as a large testbed OGS that has transmit and receive instrumentation for lunar pulse position modulation (PPM) and will include adaptive optics for quantum communication in the future [4]. A cross-continent and multi-continent optical network will be demonstrated in 2025 with joint operations of QOGS and the SSC network for CCSDS O3K downlinks. Figure 2 shows a map of these three OGS locations. SSC's collaboration with the ANU on analysis and demonstration is supported by the Australian Space Agency's Moon-to-Mars initiative, building on prior analysis conducted by SSC [5].

Figure 2: Map showing the OGS locations discussed in this paper, i.e. the SSC OGSs at WASC and Santiago and the ANU's QOGS located at Canberra. A placeholder image of the Santiago facility is shown as that OGS is not yet installed.

1.1 Concept-of-operations

SSC's optical ground segment service baseline adopts an `opportunistic' concept-of-operations (ConOps). An opportunistic ConOps means that all passes are attempted regardless of clouds, with users subscribing based on data delivered rather than traditional pass booking—which is also available for individual link tests. The non-deterministic performance of an optical service is a substantial departure from radio frequency (RF) ground segment services, i.e. GB/day and latency are variable and subject to frequent cloud outages. An optical DTE ground segment service, particularly for a sparse and preliminary network, is therefore suited for spacecraft such as Earth observation satellites that collect high volumes of data without strict latency requirements. The merits of an opportunistic approach may decrease if the utilisation rate per OGS increases, e.g. conflicting LEO passes, long GEO contacts, or limited spacecraft resources. More sophisticated ConOps may be adopted in the future which incorporate meteorology forecasts at each OGS for dynamic scheduling [6]. Extensive weather monitoring is done at both sites nonetheless, and factors such as temperature, wind speed, and rain are used for OGS automatic operations.

User spacecraft utilising this optical service are expected to conduct telemetry, tracking, and command (TT&C) with a RF ground segment. This joint system is shown in Figure 3 with spacecraft orbital elements provided by the user to the Network Management Centre (NMC). A cloud-based NMC orchestrates the optical network configuration and operations, and the received data is ultimately provided to the user with a cloud-based solution at the user interface, i.e. a GUI or API. The user interface can also be used to request OGS reconfigurations to meet differing terminals, standards, and data rates. Both OGS modems are reconfigurable to support many different missions, and possible future standard developments. This entire process is designed to be automated for both users and operators from the provision of orbital elements to data delivery. Individual passes, or a subscription of passes can be booked, with the NMC scheduling passes from provided orbital elements. Demonstrations with QOGS in 2025 will also test the process of integrating a collaborative OGS into this optical service.

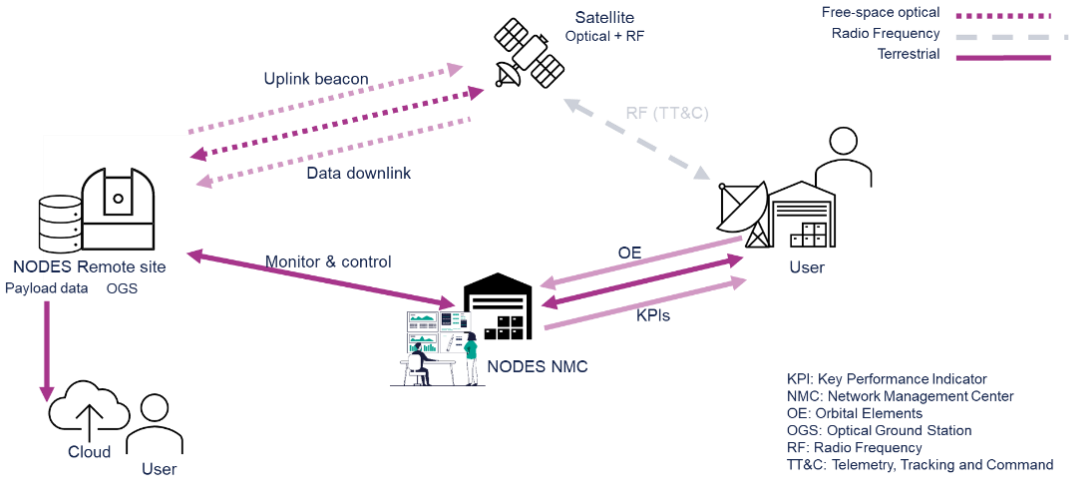

Figure 3: Graphical representation of the concept-of-operations for SSC's optical ground station network. User spacecraft transfer payload data over an optical downlink while TT&C is managed by RF antennas. The uplink optical channels are primarily needed by the satellite laser communications terminal for pointing assistance, although could also be used to transfer data and commands, as well as automatic repeat requests.

Simulating network capability is particularly important before extensive operations can provide realistic estimates. This paper is therefore focused on providing an analysis for the LEO DTE service by combining cloud cover measurements and orbital propagation simulations. Throughout the paper, the SSC optical network is considered alongside the potential benefits of collaborative operation with the ANU's QOGS. Modelling and demonstrating the benefits from collaborative OGSs is particularly important for scaling this network in the early stages. The remaining of the paper is organised as follows. Section 2 tackles the estimation of cloud cover at the OGS locations where several datasets are compared throughout yearly seasons. Next, in Section 3, a simulation analysis of the LEO DTE scenario is presented with focus on data volume and latency. Finally, modelling of a hypothetical commercial optical ground segment for lunar communications based on SSC's OGSs and QOGS is introduced in Section 4.

2. Cloud cover

Cloud cover is a critical variable to evaluate SSC's optical ground segment service, and used to estimate the service performance based on data throughput (GB/day) and latency metrics. These parameters are also relevant for comparing traditional RF communication with the new optical service. Cloud cover is estimated by analysing numerous satellite remote sensing datasets over long time spans to average out any climate variation. Table 1 summarises the seven datasets that are used to estimate cloud fraction. Cloud fraction can also be represented as the cloud-free fraction or cloud-free availability (A) which is used throughout this paper and is more directly interpretable for this application. GEO spacecraft such as Himawai-8 and assimilated datasets such as the ECMWF Reanalysis v5 (ERA5) are important for resolving spatial and temporal patterns in cloud outages which are not seen by LEO imagers such as Sentinel-2 with low revisitation rates. Spatio-temporal correlations can determine site diversity and the time scale of outages. Note that a low resolution dataset of 0.5°/pixel varies from approximately 19 km/pixel at 70°N to 56 km/pixel at the equator. An ERA5 pixel at WASCs latitude is approximately 24 km×24 km, or the area covered by 4 km base height clouds viewed above $20°$ in elevation from an OGS.

Table 1: Summary of satellite remote sensing and assimilation datasets used to measure cloud fraction.

Instrument/Dataset	Type	Time span	Spatial resolution
AHI/Himawari-8	Remote sensing	2015-2024	5 km
MODIS/Terra+Aqua	Remote sensing	2002-2024	1 km
VIIRS/SNPP	Remote sensing	2012-2024	1 km
ECMWF Reanalysis v5 (ERA5)	Assimilated dataset	1940-2024	0.25°
Landsat 5/7/8/9	Remote sensing	1984-2024	30 m
Sentinel-2	Remote sensing	2015-2024	10 m
MERRA-2	Assimilated dataset	1980-2024	0.5°

These datasets report the cloud-free availability, A, for each pixel in time which can be used to determine the statistical averages of A each month and the distribution of cloudiness, e.g. A being degraded by constant days of partial cloudiness or periods of overcast. This paper assumes that A is uniformly distributed from the viewpoint of an OGS looking $> 20°$ above the horizon, which is generally true for sites without steep terrain on spatial scales close to image resolution. This allows us to assert that the probability of cloud at zenith is equal to the all-sky time-averaged cloud fraction, e.g. a 10 m/pixel resolution dataset should converge to the same average as 24 km/pixel. Table 2 provides the annual mean of A for both SSC OGS locations and QOGS. The good agreement between datasets of differing spatial resolutions in Table 2 indicates the above assumption is appropriate for these locations. Variation between datasets is generally driven by the intricacies of cloud retrieval algorithms and sensitives to thin cloud, often considered transparent to optical links. Spatial diversity may be particularly important to consider when building regional networks, e.g. to support GEO feeder links. However, the three sites considered in this paper are far apart, such that cloud correlation is negligible on short scales and ignored here. Birch et al. (2023) presents methods to be used for modelling spatially correlated OGS networks and showed in their analysis that Canberra and WASC have a $< 5\%$ spatial correlation [7].

Table 2: Cloud-free availability for the SSC OGS locations and ANU's QOGS located in Canberra, Australia. Six datasets are included with uncertainty reported as the standard deviation from seasonal variability alone. Himawari-8 is not included for Santiago as it is not within the field-of-view for that Geostationary satellite.

	Himawari	MODIS	VIIRS	ERA5	MERRA	Landsat	Sentinel	Mean
WASC	0.73 ± 0.1	0.70 ± 0.2	0.75 ± 0.1	0.7 ± 0.1	0.76 ± 0.1	0.79 ± 0.3	0.73 ± 0.2	0.74 ± 0.2
Santiago	N/A	0.68 ± 0.2	0.71 ± 0.2	0.65 ± 0.2	0.69 ± 0.2	0.77 ± 0.3	0.72 ± 0.3	0.70 ± 0.2
Canberra	0.58 ± 0.1	0.58 ± 0.1	0.60 ± 0.1	0.48 ± 0.1	0.54 ± 0.1	0.63 ± 0.3	0.55 ± 0.2	0.57 ± 0.2

2.1 Seasonal variation

Table 2 shows that WASC and Santiago have a mean cloud-free availability of 74% and 70%, respectively, and therefore deemed as good locations for the selection for the first two SSC OGSs. Network capability must often be defined by the limiting case, e.g. to guide spacecraft requirements, so analysing seasonal variation of A is critical. Figure 4 shows the respective means of all the relevant datasets as monthly averages, highlighting that both WASC

and Santiago experience large seasonal variation with a dry summer. Seasonal temporal correlations are significant, and site diversity would be gained by adding an OGS to this network with high A during the Austral winter. Except for Landsat during the Santiago winter, all datasets shown in Figure 4 are in rough agreement within expected bounds for remotely sensed cloud cover.

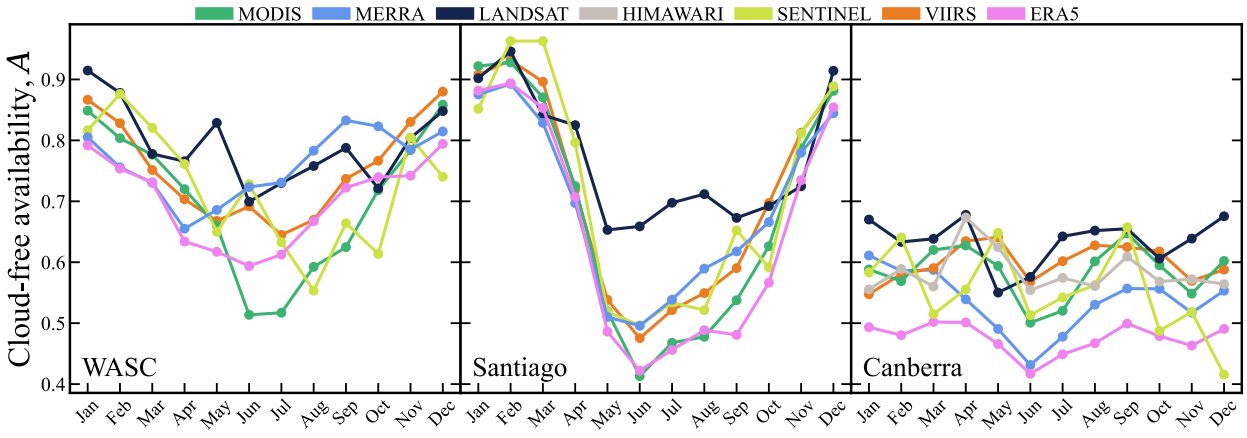

Figure 4: Monthly averages of cloud-free availability for WASC, Santiago, and Canberra. Colours represent the separate datasets outlined in Table 1.

A low average A can arise from intermittent overcast days or persistent partial cloudiness/thin cirrus, both with different implications for ConOps and latency. Figure 5 shows the seasonal variation broken into discrete degrees of cloud fraction from the ERA5 dataset for both SSC OGS locations. ERA5 determines cloud fraction from the spatial average in a pixel for a given hour, e.g. $A = 0.2$ means 80% of the 0.25°×0.25° pixel is cloudy. Figure 5 highlights how the low A during winter at Santiago is dominated by overcast days unlike WASC. An opportunistic ConOps in the absence of sophisticated weather forecasting is important for maximising throughput and latency when skies may be dominated by partial cloudiness and fractions of a link are recoverable. *In-situ* imaging of clouds is done at both WASC and Santiago with a Miratlas Integrated Sky Monitor, which may also be utilised in the future for modelling acceptable cloud thickness during links. Effective file transfer in partially cloudy conditions, i.e. intermittent links, is a relevant topic to future utilisation of delay tolerant networking for optical links.

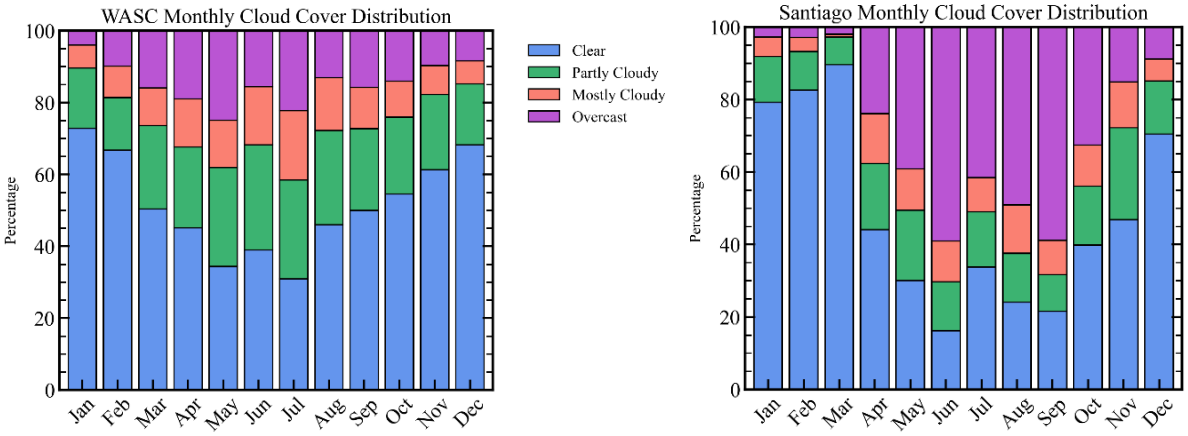

Figure 5: Monthly distributions of cloud cover determined from the ECMWF Reanalysis v5 dataset. Cloud cover is categorised by the cloud-free availability, A, of each site's pixel. Overcast is considered $A < 0.2$ mostly cloudy is $0.2 < A < 0.5$, partly cloudy is $0.5 < A < 0.9$, and clear is considered $A > 0.9$.

3. Low Earth Orbit Direct-to-Earth scenario

SSC's optical ground segment service is focused on DTE links from LEO spacecraft. Earth observation spacecraft in Sun-synchronous orbit (SSO) are envisioned as likely users of this service because of the large volumes of data

collected and the typically looser requirements on latency than other applications. Modelling the capability of these OGSs is approached by simulating a fiducial LEO spacecraft in a 550 km SSO with the `Orekit` package [8]. $\theta_{elevation} > 20°$ is used as the requirement for contacts throughout this section, with glancing passes that do not rise above 25° ignored. The remaining of this section focuses on estimating the aforementioned key performance parameters for the optical ground segment service: data volume (GB/day) and latency (minutes).

3.1 Data volume estimation

Orbital propagation is combined with cloud-free availability measurements to estimate the data throughput of SSC's optical service. Simulated propagation converges on a statistical average of contact time for links with $\theta_{elevation} > 20°$ expressed in minutes per day. This ignores link time lost during acquisition and deep fades, among other possible inefficiencies. Contact time averages can be scaled by A to correct for outages each month as plotted in Figure 6. This also relies on an assumption that the successful fraction of a pass is equivalent to A, partly a product of the opportunistic ConOps for this service (ignores performance degradation in mostly cloudy conditions shown as orange of Figure 5). Contact time in Figure 6 is also expressed as daily data volume provided to the user with the SDA 4.0 OCT standard of 2.5 Gbps with 0.76 code rate, i.e. a user data rate of 1.73 Gbps [3].

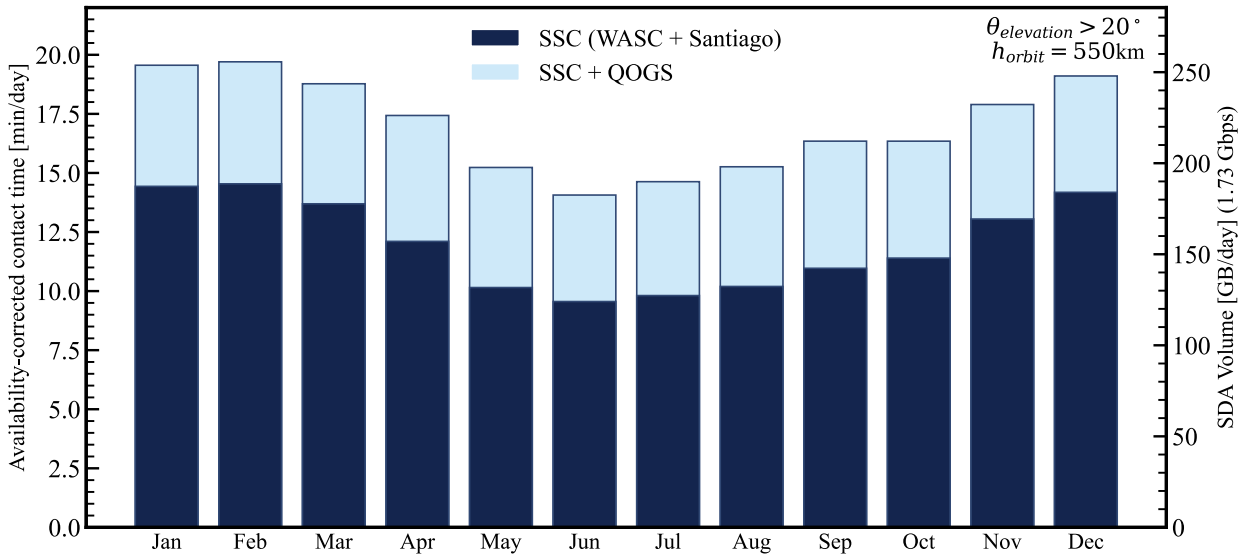

Figure 6: Average daily contact times and data volume as a function of month for SSC OGSs and addition of ANU's QOGS. Contact time estimates are computed for spacecraft in 550 km near-polar SSO. Daily data volume computed by scaling contact time by data rate. SDA OCT 4.0 standard of 2.5 Gbps with 0.76 code rate for 1.73 Gbps user data rate is used.

Figure 6 highlights that a preliminary service of two OGSs, far from the poles, can still throughput >120 GB/day on average during the low availability winter months. Crucially, these volumes are possible with very small spacecraft terminals and no spectrum regulation. Furthermore, if ANU's QOGS is included in the network the minimum during June of 9.6 mins/day increases to 14.1 mins/day. If a spacecraft can establish 10 Gbps links, the current limit of SSC OGSs, data throughput can exceed a TB/day. Note that these sites are not in locations optimised for polar orbits, unlike arctic RF ground stations that can establish contact on every orbit. Contact time and data throughput is strongly a function of orbital inclination and Figure 7 presents the annual average of contact time and data volume as a function of spacecraft inclination from 20° to 100°. Figure 7 estimates contact time by using the annual average of A shown in Table 2, with the spacecraft having a fixed altitude of 550 km and links taking place with $\theta_{elevation} > 20°$. The International Space Station (ISS) is inclined at 51° and Figure 7 shows that contact time in that orbit would be approximately 50% greater than SSO (≈ 98°) for this network.

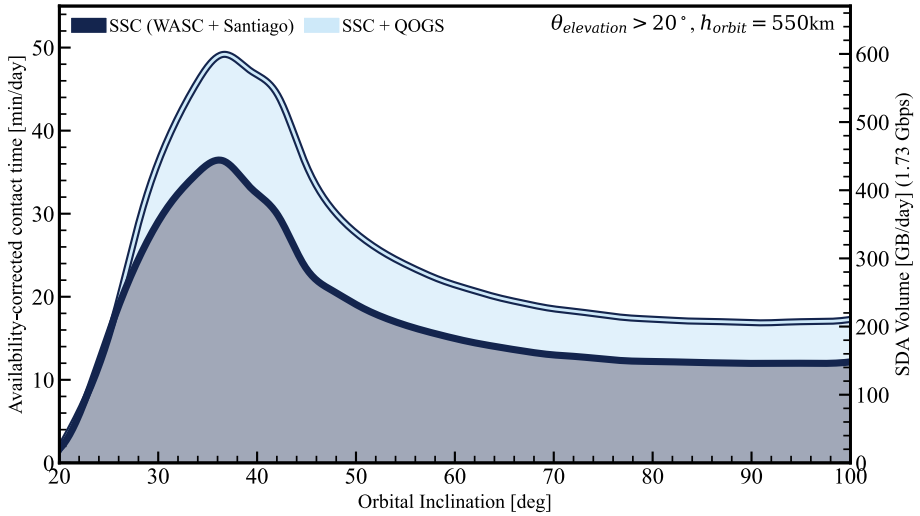

Figure 7: Contact time as a function of orbital inclination for simulated 550 km LEO spacecraft. Contact time is estimated by scaling the output of orbital propagation by the annual mean of cloud-free availability determined from a range of datasets. Results are shown for both SSC's two OGS network and the addition of ANU's QOGS. Date volume is based on data rate from SDA OCT 4.0 standard of 2.5 Gbps with 0.76 code rate, i.e. a user date rate of 1.73 Gbps.

3.2 Latency

Data volume estimates do not capture the length or frequency of outages imposed by a sparse optical network. Outages define the uncertainty in throughput performance, and the typical latency provided by the network. Modelling latency is not only important to understand the performance capability of a data repatriation service, but also to inform a future expansion of a network. The latency of SSC's optical ground network is estimated in two ways. Firstly, a spacecraft in 550 km SSO is propagated for three years, and each contact is considered successful or failed by Monte Carlo sampling a Bernoulli distribution of A. The Bernoulli distribution does not model performance in partly or mostly cloudy conditions, and a Monte Carlo method does not capture temporal correlations as the chance of cloud is independent between passes. The results of this simulation are used to compute a map of latency shown in Figure 8, also providing a visual aid to where future OGSs might be placed to minimise latency.

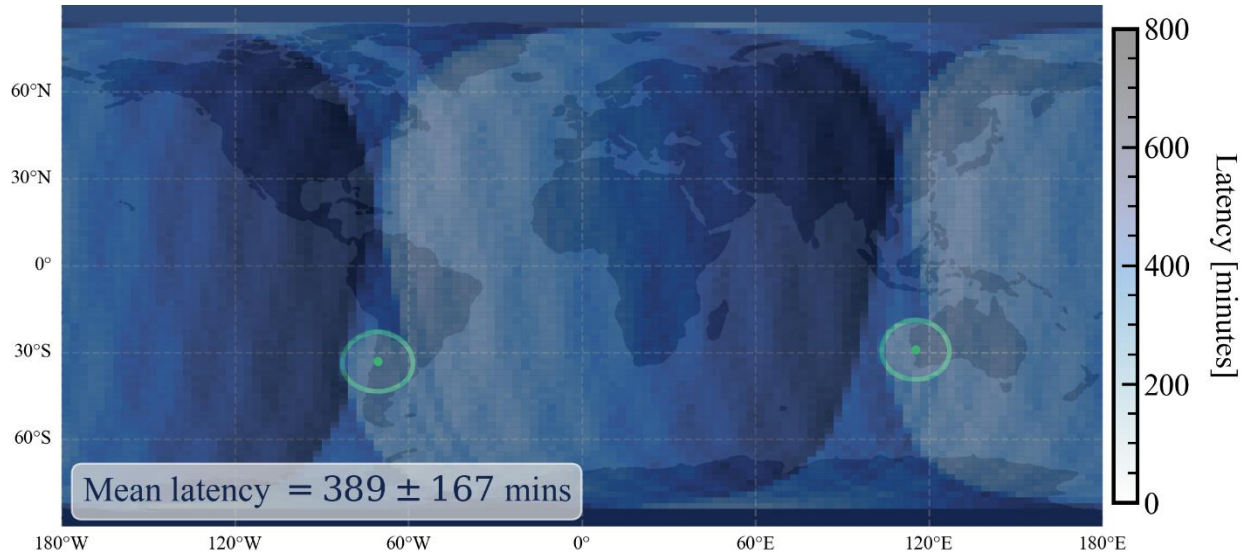

Figure 8: Spatial map of latency for SSC optical ground network to Sun-synchronous satellite at 550 km. Annual estimates of cloud-free availability are used to determine the fraction of missed passes. The spatial average of this annual estimate is annotated in the lower left corner with uncertainty representing the spatial standard deviation.

The spatio-temporal latency average based on the annual estimates of A is shown in Figure 8 as 389 ± 167 minutes. This large value of approximately six and a half hours highlights that this network is not optimised for SSO, and more stations are needed to improve the service and fully leverage optical for this application. Unfortunately, Arctic locations that typically service polar orbiting satellites do not have favourable climates for optical communication so expansion should rather focus on dry sites spaced in longitude. Figure 9 shows the result of repeating this process as a function of monthly A, and the improvement from adding QOGS to the network. A moderate network expansion to 4 or 5 sites could bring this average below two hours, while significantly boosting throughput.

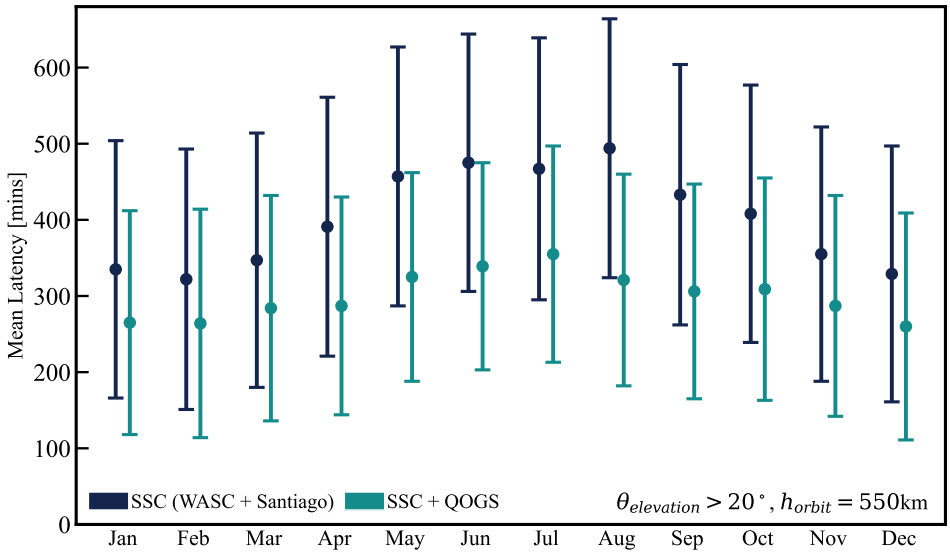

Figure 9: Monthly statistical means of the spatial latency. Values represent typical latencies for a Sun-synchronous spacecraft at an orbital height of 550 km. Latency to the SSC network of WASC and Santiago are provided alongside the addition of ANU's QOGS to the network.

A second approach to estimate network latency is also presented in this paper, because the Monte Carlo approach does not maintain important information on the temporal scale of cloud cover or the distribution of latencies. Four years of hourly data from ERA5 at each site spanning 2021 to 2024 is mapped against four years of orbital propagation contacts to build a realistic history of network performance. This data is used to study the typical gaps between passes, with Figure 10 showing the histogram of these gaps for both a 550 km satellite in SSO, and the ISS. This approach only considers the SSC network of WASC and Santiago and ignores QOGS. Passes are excluded that last less than 40 s or do not rise above 25° in elevation. Figure 10 also constrains the x-axis for readability and does not show the very few incidences when gaps > 30 hrs occur because of lingering concurrent cloudiness at both sites (less than 1% of gaps between passes are greater than 30 hours over the simulation). Pass gaps for the simulated spacecraft in SSO are on average 550 minutes (2.5 hours longer than the first approach) but are bimodally distributed around 45 minutes or 11 hours. Short gaps of around 45 minutes occur when the spacecraft flies over the South pole and quickly establishes a second contact if both sites are cloud free, highlighted in Figure 10.

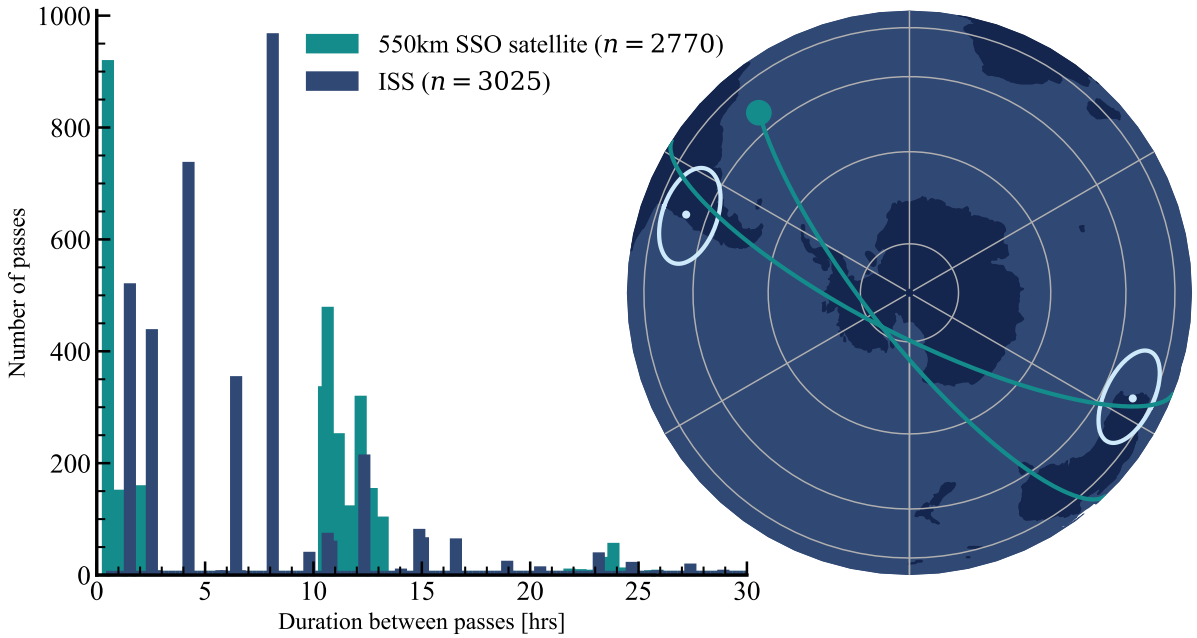

Figure 10: Left: Histograms of the gaps between passes for the SSC optical ground network of WASC and Santiago indicative of latency for LEO ground segment service. Results are constructed from four years of hourly cloud data combined with orbital propagation of the ISS and a theoretical spacecraft in a 550 km SSO. The low number of pass gaps longer than 30 hours are excluded for readability. Right: Polar projection of WASC and Santiago coverage with the ground track of an SSO spacecraft in green to highlight the common occurrence of <1 hr latency visible in the histogram. The OGS field-of-view projection coverage to 550 km with $\theta_{elevation} > 20°$ is shown for both OGS locations in white.

3.3 Performance summary for Sun-synchronous orbit

Statistical estimates of the contact time (12 minutes/day), latency (401 minutes) and data volume (156 GB/day) for the SSC network are provided in Table 3. Additionally, the SSC and QOGS are incorporated showing an increased performance of around 40% for contact time and data volume, and a reduction of around 25% in latency. All values are provided for the theoretical satellite in a 550 km SSO which has been simulated throughout, and cloud-free availabilities from the aggregated datasets in Section 2. Values provided represent the annual average with uncertainty bounds from the best and worst performing months, i.e. highest and lowest A respectively.

Latency in Table 3 refers to the Monte Carlo results from Figure 9 (Figure 8 average is slightly different as simulations are not strictly converged). The uncertainty of latency is the norm of seasonal minima/maxima bounds and spatial standard deviation. Strong differences among the distribution of time between passes in Figure 10 and the latency results in Table 3 are observed. Those may be attributed to link performance through thin cirrus cloud, partially cloudy conditions, and elevation angles $< 20°$. Further refinement to the model is expected with early operation of the service.

Table 3: Summary of optical ground segment service capability for DTE links from a LEO spacecraft in 550 km SSO. SDA data volume is computed from a user data rate of 1.73 Gbps (0.76 code rate) [3]. Uncertainty bounds for contact time and SDA data volume are the averages of the minimum and maximum bounds from monthly variation. Uncertainty for latency is the norm of spatial standard deviation and monthly minimum/maximum bounds.

Network	Contact time [mins/day]	Latency [mins]	Data volume [GB/day]
SSC (WASC + Santiago)	12.0 ± 2.5	401 ± 190	156 ± 32
SSC + QOGS	17.0 ± 2.8	300 ± 151	221 ± 37

4. Lunar optical ground segment

Hybrid optical/RF architectures based on delay tolerant networking are expected to become the communications backbone of the future lunar economy [9, 10]. Lunar spacecraft will proliferate over the next ten years, and SSC has

already established its capability to provide a lunar RF ground segment for commercial payloads as recently as Firefly's Blue Ghost lander in Q1 2025 [11]. The advantages of optical links over RF scale well into deep space, and optical communication has therefore garnered significant interest in its future role of the lunar communications landscape [10]. The Optical-to-Orion (O2O) terminal on the Artemis II mission in 2026 will be the second demonstration of lunar optical communication following the *Lunar Laser Communication Demonstration* in 2013, which conducted downlinks at 622 Mbps [12]. O2O is capable of approximately 250 times the data rate of the S-band link on the Orion spacecraft, highlighting the potential for optical communications in deep space. QOGS is being upgraded with instrumentation for lunar PPM links such as used by O2O, despite SSC OGSs only currently supporting LEO links [4]. In this section we present network availability results from a hypothetical optical ground network for lunar communications consisting of three facilities, and in Section 5.1 the first results of a hybrid optical/RF DTN simulation to estimate onboard data storage offloading.

Figure 11 shows the OGS field-of-view projection coverage for lunar distance for elevation angles down to 20° for the three OGS considered in this paper in white, and the shaded region that covers the moon's ground track over its cycles in green. Performance of a lunar optical network can be parametrised by network availability, i.e. probability of uptime in comparison to the $> 99\%$ from three equidistant antennas in a typical deep-space RF network. Network availability is estimated by taking average contacts to the Moon per day for all sites and scaling those by annual estimates of A. For example, WASC may have a 9 hr contact per day to the Moon which is reduced by cloud cover to an average of 6.6 hours per day or an annual average of 28% network availability. Typical daily contacts are also plotted in Figure 11 as a function of time for one day, showing gaps and overlaps averaged over lunar cycle variation. Overlapping contacts represent mutual visibility or site diversity, that is critical in boosting reliability. The network availability where two OGSs maintain mutual visibility is computed by assuming 0 spatial correlation (see [7]). Figure 11 also equates visibility to the Moon as visibility to a spacecraft, appropriate if representing a future constellation such as the Moonlight programme or spacecraft in near-rectilinear halo orbit such as the Lunar Gateway.

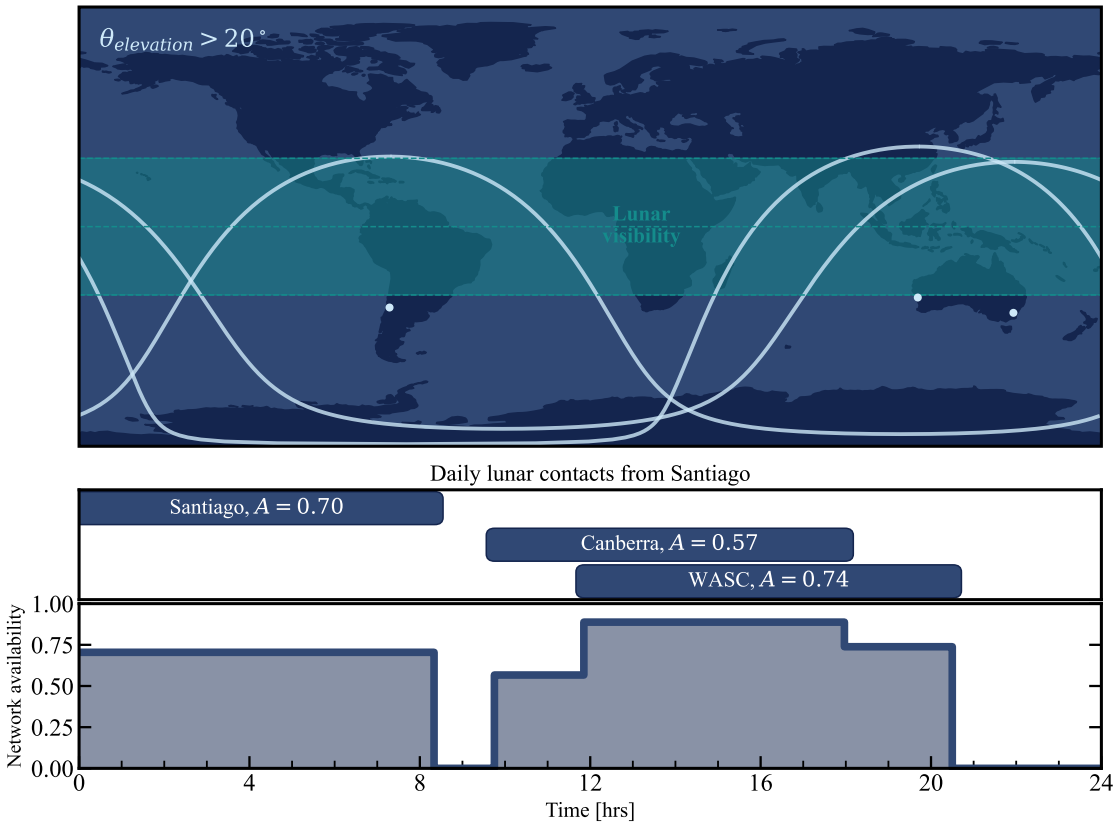

Figure 11: Optical ground segment for lunar optical communication. Top: Coverage for three OGS network shown in white based on $\theta_{elevation} > 20°$. Shaded green area represents the lunar ground track region that is covered over lunar cycles. Bottom: optical network coverage as a function of time for a standard period of 24 hours and contact durations averaged over all lunar and seasonal variation. Step function scales contacts by cloud-free availability to represent network-wide availability, and computes outage probability in overlapping visibilities.

The lower inset in Figure 11 shows the network availability as a function of time over an average day, incorporating mutual visibility into the increased reliability. Integrating over time yields a total efficiency of the network with respect to 100% uptime per day. The network of WASC, Santiago, and Canberra therefore has a network availability of 60% or an annual average of 14.5 hrs/day. Statistics on the gaps between lunar links can also be assessed in a similar way as with LEO spacecraft in Section 4, as Figure 11 does not strictly capture mutual outage probabilities. Histograms of these lunar network outages are shown in Figure 12, for the network of WASC, Santiago, and Canberra. Additionally, Figure 12 shows with and without the presence of clouds to show how degradation adds a tail to the distribution. The median from the distributions in Figure 12 corresponds to the gap visible over Europe and Africa shown in Figure 11.

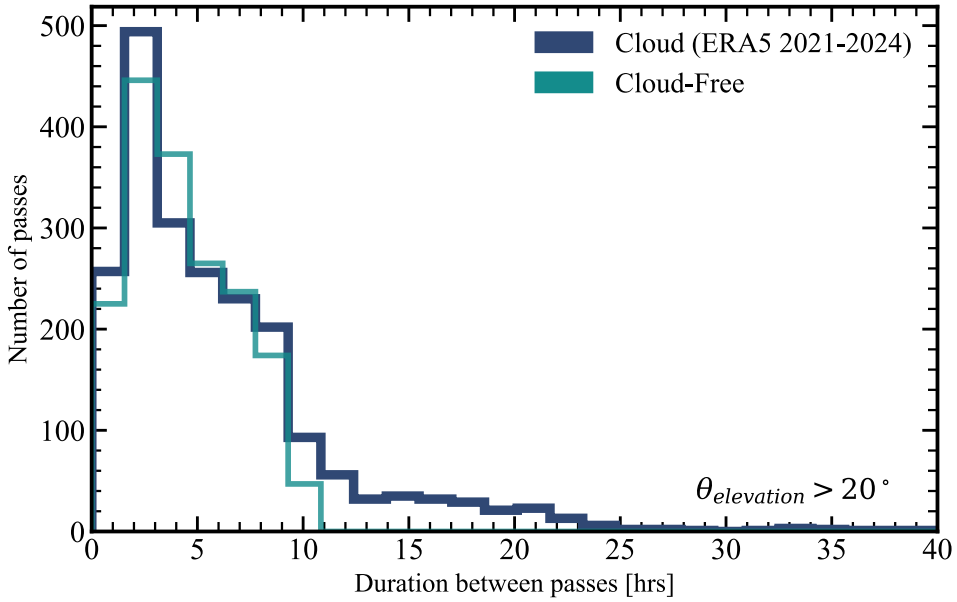

Figure 12: Histogram for gaps between lunar contacts for optical network of WASC, Santiago and Canberra. Outage durations are computed with orbital propagation and the cloud fraction time series from ERA5 dataset.

5.1 Delay tolerant networking simulations

Dedicated communications spacecraft or constellations at the Moon will facilitate complex multi-hop networks to support the future lunar economy [10]. Delay tolerant networking (DTN), such as set out in the LunaNet interoperability specification, will be critical for supporting these future networks [9]. A DTN implements bundle protocol with software on each node to facilitate a dynamic store-and-forward communications architecture. Optical communications is well-suited to adopt DTN given the dominance of unscheduled outages from cloud cover, and atmospheric deep fades that may be similar in time to propagation delay at lunar distances. The on-board storage of an orbiter such as Gateway will act as a store-and-forward node for other assets such as lunar landers and rovers when the optical ground segment is blocked by clouds. DTN can also combine bundles received from numerous intermittent sources with unknown propagation delay, maximising throughput and simplifying operational overheads. An optical ground segment can therefore benefit from being operated in a hybrid DTN with a RF ground segment that can receive payload data during optical outages in addition to the requisite TT&C.

The `DTNSim` package for `OMNET++` is used to study a hybrid optical/RF lunar DTN scenario [13]. The Lunar Gateway's 100 Mbps K_a band capability is simulated in addition to a theoretical 622 Mbps optical link based on the data rate achieved in 2013 with the *Lunar Laser Communication Demonstration* [12]. This ignores any channel coding and simplifies orbital dynamics by holding to the prior assumption that the Lunar Gateway is always in view of a ground station when the Moon is visible. Future constellations in lunar orbit such as ESA's Moonlight programme should also satisfy this criteria. WASC and Santiago are the modelled optical ground segment in this scenario, omitting QOGS. The RF ground segment has a 100% uptime, and could therefore represent any number of networks such as SSC's global lunar network or NASAs Lunar Exploration Ground Sites. This simple network focuses on modelling DTE outages rather than multi-hop space link networks. The optical contact plan is generated in the same manner as the prior study of outage durations using hourly ERA5 data (Figure 10 & Figure 12). This contact plan is then provided to `DTNSim` and the discrete event simulation is run to model the transfer of bundles from the lunar spacecraft to the

network operations centre. Figure 13 shows the on-board storage during this simulation with a constant and arbitrary 264 Mbps data accumulation rate. Stored data can fluctuate past 10 TB with consecutive OGS outages and the moon at low elevation angles, showing the importance of implementing store-and-forward nodes with DTN. Figure 13 also highlights data throughput from a small optical ground network based on optical capabilities from 2012 [12].

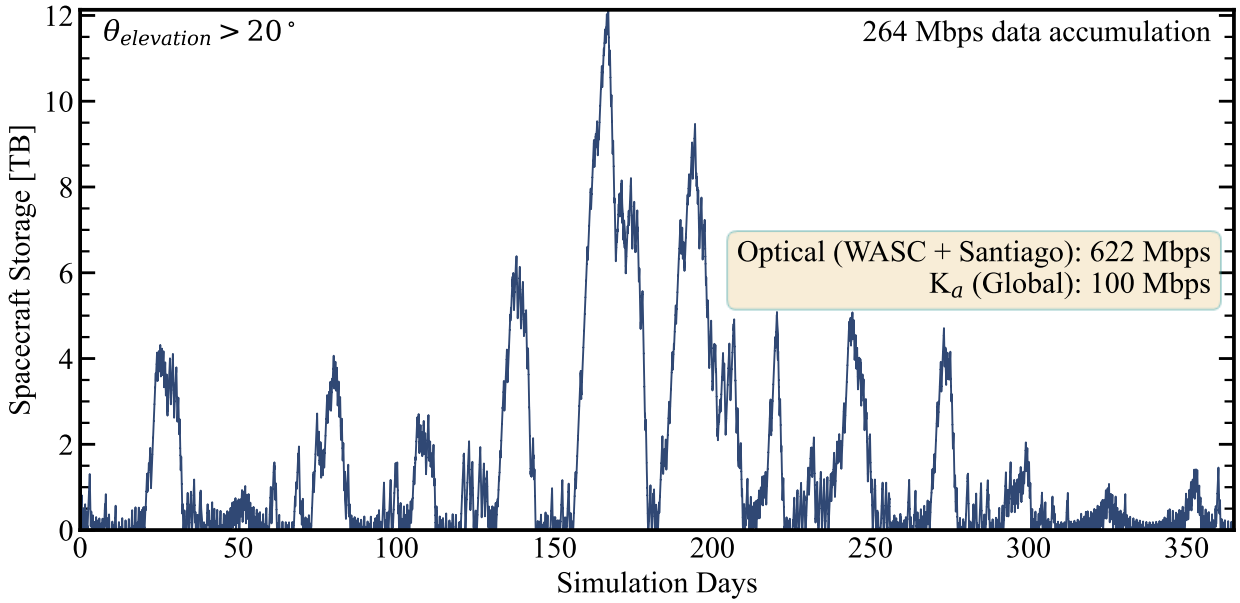

Figure 13: Simulated on board storage for lunar spacecraft over one year, with a data accumulation rate of 264 Mbps. `DTNSim` package for `OMNET++` is used to produce the result, simulating a hybrid RF/optical ground segment [13].

SSC OGSs could be upgraded to offer a commercial lunar optical ground segment once the requirements of future missions are better understood. Future lunar optical terminals, after O2O, will determine the complexity of upgrades for such a service, e.g. photon-counting PPM or coherent links with adaptive optics. Further simulations will also be used to model the DTN protocol stack and study LunaNet implementation for SSCs optical network.

5. Conclusion

SSC is establishing one of the first commercial offerings of an optical ground segment service. This capability will transform data transfer for LEO spacecraft and demonstrate the technological readiness of space-to-ground optical communications. Analysis has been presented to show that SSCs network of two OGSs will be capable of delivering over 200 GB/day with the 2.5 Gbps SDA standard from LEO, and volume could be increased by 40% in collaboration with QOGS. SSC OGSs are also capable of 10 Gbps and can be upgraded in the future to grow with the rapid pace of development and data rates. SSC and the ANU will demonstrate this collaborative network in 2025 with the automated booking and user interface developed in the NODES project. Latency in the existing network can range from 4 to 10 hours on average, given the small size of the network, but future expansion of this optical ground segment beyond 3 OGSs will further leverage the technology and support many TB/day at lower latencies. SSC's commercial optical ground segment for LEO links will offer a novel capability while also demonstrating readiness for the future growth of this technology such as lunar optical communication. This paper also highlighted the capability of a lunar optical ground segment, in collaboration with the ANU, by combining weather data with DTN simulations and orbital dynamics.

Acknowledgements

The NODES project is partly supported by the Swedish National Space Agency (SNSA) through the European Space Agency ARTES ScyLight programme. SSC and the ANU acknowledge the Australian Space Agency for supporting this research and collaboration through the Moon-to-Mars Initiative Demonstrator Mission Grant.

References

[1] CCSDS, "Draft Optical Communications Physical Layer, CCSDS 141.0-P-1.1," July 2020. [Online]. Available: https://public.ccsds.org/Lists/CCSDS%201410P11/141x0p11.pdf.

[2] CCSDS, "Draft Non-Coherent Optical Communications Coding and Synchronization 142.0-P-1.1," November 2023. [Online]. Available: https://public.ccsds.org/review/CCSDS%20142.0-P-1.1/142x0p11.pdf.

[3] SDA, United States Space Force, "Optical Communications Terminal (OCT) Standard Version 4.0," 28 June 2024. [Online]. Available: https://www.sda.mil/wp-content/uploads/2024/07/SDA_OCT_Standard_4.0.0_final-20240701.pdf.

[4] M. Copeland, F. Bennet, M. Birch, K. Ferguson, D. Grosse, E. Jager, N. M. Rey and T. Travouillon, "Deep space communication with the ANU optical communications ground station," *Free-Space Laser Communications XXXVI,* vol. 12877, pp. 370--376, 2024.

[5] H. Sundberg, M. Sans, P. Pasuwan and P. Hyvönen, "Development of an Optical Communication Ground Network for Direct-to-Earth Data Repatriation Service," in *International Conference on Space Operations*, 2023.

[6] A. Furbacher, T. Fruth, A. Wiebigke, M. T. Worle, F. Mrowka, K. Saucke, M. P. Patricia and M. Knopp, "Concept for generic agile, reactive optical link planning," *CEAS Space Journal,* 2025.

[7] M. Birch, J. R. Beattie, F. Bennet, N. Rattenbury, M. Copeland, T. Travouillon, K. Ferguson, J. Cater and M. Sayat, "Availability, outage, and capacity of spatially correlated, Australasian free-space optical networks," *Journal of Optical Communications and Networking,* vol. 15, no. 7, pp. 415--430, 2023.

[8] Orekit PMC, "CS-SI/Orekit: 12.2.1," Zenodo, 18 December 2024. [Online]. Available: https://doi.org/10.5281/zenodo.14520271.

[9] NASA and ESA, "LunaNet Interoperability Specification Document Version 4," 12 09 2022. [Online]. Available: https://www3.nasa.gov/sites/default/files/atoms/files/lunanet_interoperability_specification_version_4.pdf. [Accessed 08 10 2024].

[10] Interagency Operations Advisory Group, "Report of the Lunar Communications Architecture Working Group on The Future Lunar Communications Architecture V1.3," 22 01 2022. [Online]. Available: https://www.ioag.org/Public%20Documents/Lunar%20communications%20architecture%20study%20report%20FINAL%20v1.3.pdf. [Accessed 08 10 2024].

[11] Swedish Space Corporation, "SSC Supports Firefly Aerospace's Blue Ghost Mission to the Moon," 14 January 2025. [Online]. Available: https://sscspace.com/ssc-supports-firefly-aerospaces-blue-ghost-mission-to-the-moon/.

[12] D. M. Boroson, B. S. Robinson, D. V. Murphy, D. A. Burianek, F. Khatri, J. M. Kovalik, Z. Sodnik and D. M. Cornwell, "Overview and results of the lunar laser communication demonstration," *Free-Space Laser Communication and Atmospheric Propagation XXVI,* vol. 8971, pp. 213-223, 2014.

[13] J. A. Fraire, P. Madoery, F. Raverta, J. M. Finochietto and R. Velazco, "Dtnsim: Bridging the gap between simulation and implementation of space-terrestrial DTNs," in *2017 6th International Conference on Space Mission Challenges for Information Technology (SMC-IT)*, 2017.

[14] NASA Human Exploration and Operations Mission Directorate, "International Communication System," 09 2020. [Online]. Available: https://internationaldeepspacestandards.com/wp-content/uploads/2024/02/communication_reva_final_9-2020.pdf. [Accessed 10 10 2024].

[15] The Consultative Committee for Space Data Systems, "CCSDS Recommendation for Optical Communications Physical Layer CCSDS 141.0-B-1," 08 2019. [Online]. Available: https://public.ccsds.org/Pubs/141x0b1.pdf. [Accessed 08 10 2024].

[16] The Consultative Committee for Space Data Systems, "Draft Recommendation for Non-Coherent Optical Communications Coding and Synchronization CCSDS 142.0-P-1.1," 11 2023. [Online]. Available: https://public.ccsds.org/review/CCSDS%20142.0-P-1.1/142x0p11.pdf. [Accessed 08 10 2024].

[17] The Consultative Committee for Space Data Systems, "Draft Recommendation for Optical Communications Physical Layer CCSDS 141.0-P-1.1," 07 2020. [Online]. Available: https://public.ccsds.org/Lists/CCSDS%201410P11/141x0p11.pdf. [Accessed 08 10 2024].

[18] The Consultative Committee for Space Data Systems, "Recommendation for Optical Communications Coding and Synchronization CCSDS 142.0-B-1," 08 2019. [Online]. Available: https://public.ccsds.org/Pubs/142x0b1.pdf. [Accessed 08 10 2024].